TUCAN

Development of high-performance UCN polarization analyzers at J-PARC and JRR-3

nEDM2023 - The 5th Workshop on Searches for a Neutron Electric Dipole Moment

2023-11-07

Takashi Higuchi (KURNS*, Kyoto Univ.)
for the TUCAN collaboration and M. Hino

*KURRI → KURNS (2018)

Outline

- Introduction
  - Principle
  - Review of previous works
  - Our motivations
  - Test methods: UCN transmission measurement, cold-neutron reflectometry
- Recent results
  - UCN measurement at J-PARC
  - Cold-neutron reflectometry measurement at JRR-3
- Summary

Principle

- UCN interaction with magnetic material:

$$V_{\mathrm{eff},\pm} = V_F \pm |\boldsymbol{\mu}_\mathbf{n}| \cdot \mathbf{B} = 209\ \mathrm{neV}\ \pm 60\,\frac{\mathrm{neV}}{\mathrm{T}} \cdot B \quad \text{(for Fe)}$$

- Magnetized Fe films (~2 T) (V_+=329 neV, V_-=89 neV) ⇒ UCN polarizers
- Used together with spin flippers and detectors ⇒ UCN spin analyzers
- Fidelity of spin-state identification directly influences the visibility of the Ramsey fringes

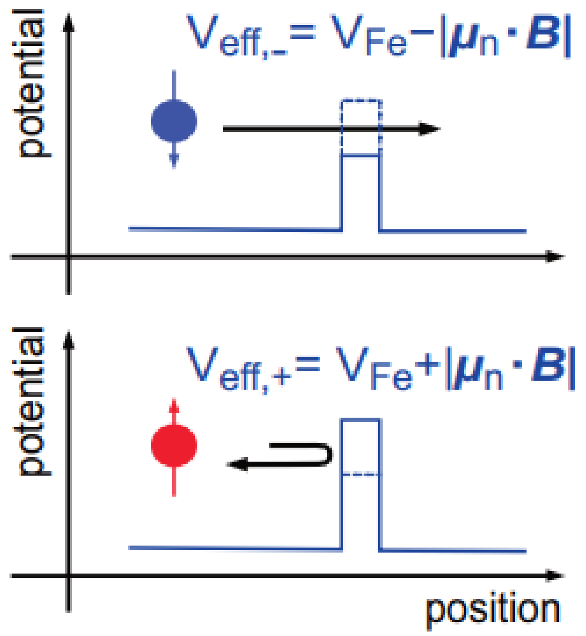

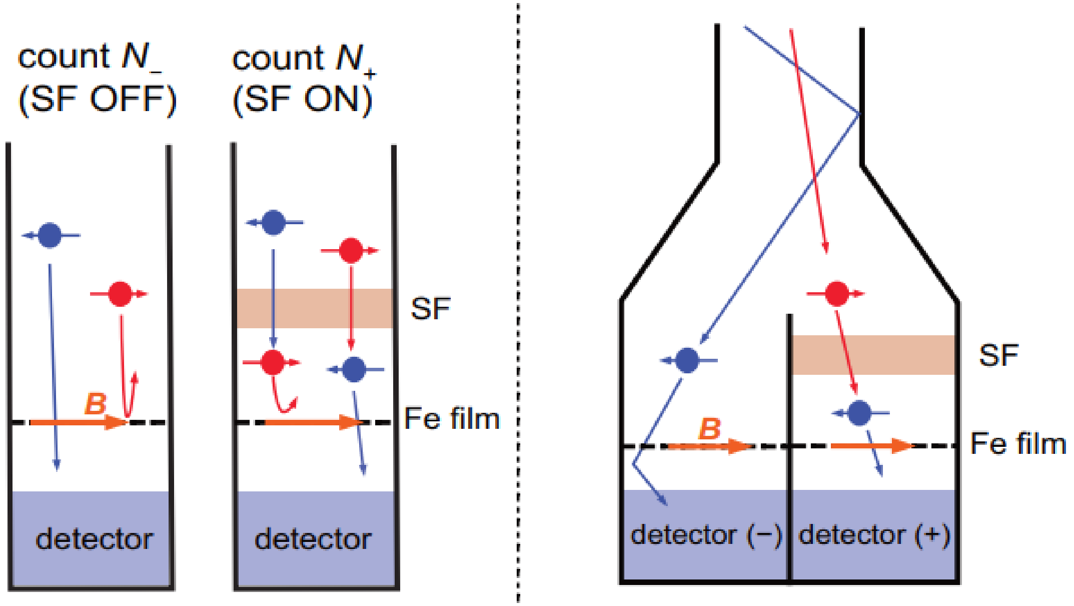

simultaneous spin analyzer: S. Afach *et al.*, EPJ A **51**, 143 (2015)

Review of previous works

- State-of-the art performance: ≥ 0.90
- Sputtering vs vacuum deposition:
  - Sputtering became more common.
  - Advantages:
    strong adherence of film, thin layers possible (→ low absorption)
- Common substrates: Al or Si
- Magnetic field used:
  vary from ~10 mT to ~100 mT
  - In principle, fully magnetized films are fine
  - Can confirm the performance only after UCN measurement
  - Permanent magnet system required for high field

Authors (year)	Mtehod	Substrate	Fe thickness (nm)	Magnetic field (mT)	Polarization
Egorov et al. (1974)	VD	Ti (1.5 um) / cover glass (100 um)	200	?	p'=0.75
Herdin et al. (1978)	VD	NaCl	150 / 300	60	p = 0.95 (2) / 0.98 (3)
Rogel (2009)	VD/IBS	Al foil (13-100 um)	200-1000	40	p=0.90
Lauer (2012)	IBS	Al foil	150	10	p=0.96 (3)
Hélaine (2014)	VD/IBS	Al foil (25 um)	400	120	p'= 0.90 (3), 0.91 (3)
Baker et al. (2014)	VD	Si	1000	100	?
Zechlau (2016)	MS	Si	300	10	p'=0.96 (3)
Zechlau (2016)	MS	FeSi (supermirror)	15.3-128 (supermirror)	10	p'=0.99 (2)
Schreyer (2017)	MS	Al foil (100 um)	150	27	p=0.960 (8)

VD: vacuum deposition
IBS: ion-beam sputtering
MS: magnetron sputtering

p, p': see next page

- **We propose polarized cold neutron reflectometry as a test method of Fe films complementary to UCN tests**

UCN transmission measurement

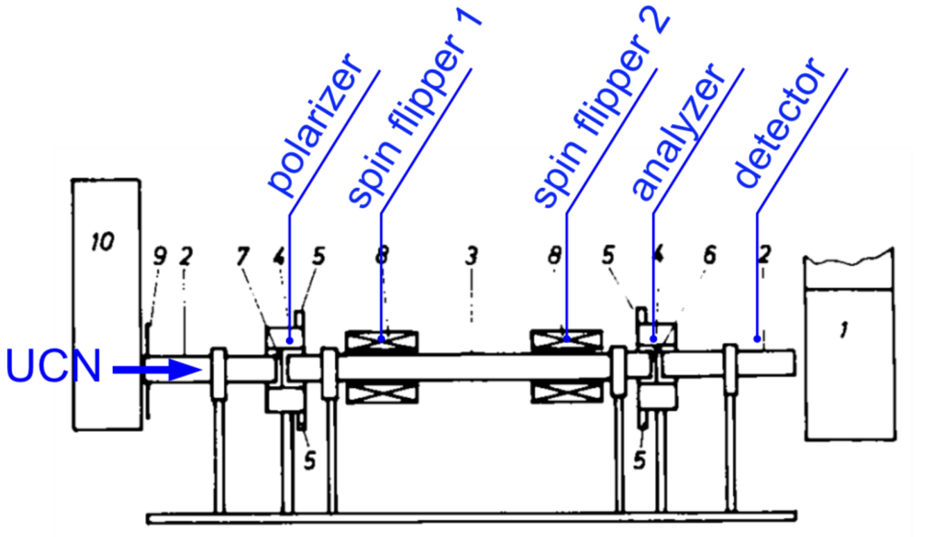

R. Herdin et al. NIM A **148**, 353(1978)

- Matrix formalism

  Basis: $|-\rangle = \begin{pmatrix} 1 \\ 0 \end{pmatrix}, \; |+\rangle = \begin{pmatrix} 0 \\ 1 \end{pmatrix}$

  Polarizer/analyzer: $A = \begin{pmatrix} a_{11} & a_{12} \\ a_{21} & a_{22} \end{pmatrix}$, ideally: $\begin{pmatrix} 1 & 0 \\ 0 & 0 \end{pmatrix}$

  Detector: $D = \begin{pmatrix} 1 & 1 \end{pmatrix}$, SFs: $F_1 = \begin{pmatrix} \epsilon_1 & 1-\epsilon_1 \\ 1-\epsilon_1 & \epsilon_1 \end{pmatrix}, \; F_2 = \begin{pmatrix} \epsilon_2 & 1-\epsilon_2 \\ 1-\epsilon_2 & \epsilon_2 \end{pmatrix}.$

- Experimental observables: (SF1, SF2)=(0,0), (0,1), (1,0) ,(1,1) → 6 unknown parameters for 4 exp. configs

$$N_{ij} = DA(F_2)^j (F_1)^i A \begin{pmatrix} 1 \\ 1 \end{pmatrix} \quad (i, j \in \{0, 1\})$$

- Assumptions on *A:*
  - *Herdin et al.*

    $$A = \begin{pmatrix} a_{11} & 0 \\ a_{21} & 0 \end{pmatrix} \Rightarrow p = \frac{a_{11}}{a_{11} + a_{21}} = \frac{N_{00} - N_{10}}{f_1 \cdot N_{00} + N_{10}}; \; f_1 = \frac{N_{11} - N_{10}}{N_{00} - N_{01}}$$

  - *Egorov et al.*

    $$A = \begin{pmatrix} a_{11} & 0 \\ 0 & a_{22} \end{pmatrix} \Rightarrow p' = \frac{a_{11}}{a_{11} + a_{22}} = \sqrt{p}$$

J. Byrne, NIM A 167, 355 (1999) :

The assumption of Herdin et al.needs to different polarization vector amplitudes between polarizer (p) and analyzer (1).

The assumption of Egorov et al is more natural

⇒ UCN transmission experiment cannot fully distinguish different mechanisms of depolarization

UCN transmission measurement

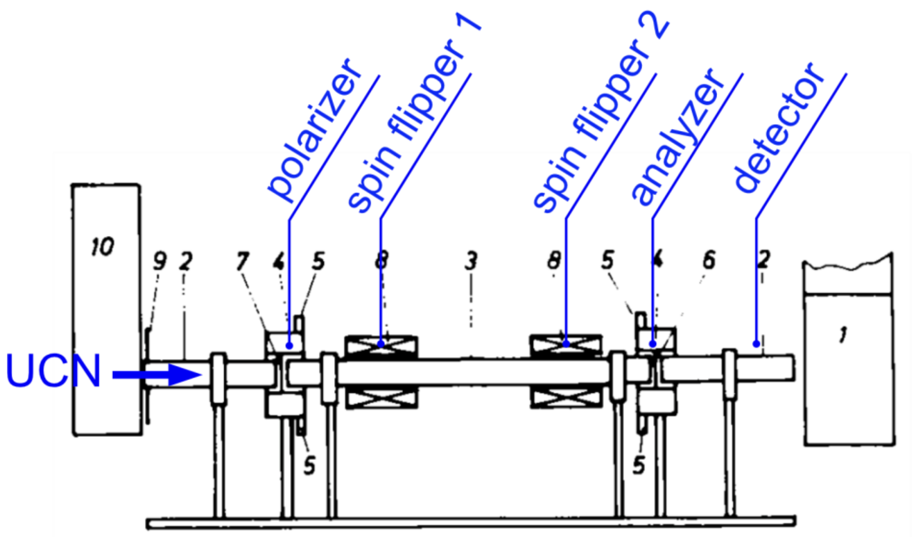

R. Herdin et al. NIM A **148**, 353(1978)

- Matrix formalism

  Basis: $|-\rangle = \begin{pmatrix}1\\0\end{pmatrix},\ |+\rangle = \begin{pmatrix}0\\1\end{pmatrix}$

  Polarizer/analyzer: $A = \begin{pmatrix}a_{11} & a_{12}\\ a_{21} & a_{22}\end{pmatrix}$, ideally: $\begin{pmatrix}1 & 0\\ 0 & 0\end{pmatrix}$

  Detector: $D = \begin{pmatrix}1 & 1\end{pmatrix}$, SFs: $F_1 = \begin{pmatrix}\epsilon_1 & 1-\epsilon_1\\ 1-\epsilon_1 & \epsilon_1\end{pmatrix},\ F_2 = \begin{pmatrix}\epsilon_2 & 1-\epsilon_2\\ 1-\epsilon_2 & \epsilon_2\end{pmatrix}.$

- Experimental observables: (SF1, SF2)=(0,0), (0,1), (1,0), (1,1) → 6 unknown parameters for 4 exp. configs

$$N_{ij} = DA(F_2)^j(F_1)^iA\begin{pmatrix}1\\1\end{pmatrix} \quad (i, j \in \{0,1\})$$

- Assumptions on *A:*
  - *Herdin et al.*

    $$A = \begin{pmatrix}a_{11} & 0\\ a_{21} & 0\end{pmatrix} \Rightarrow p = \frac{a_{11}}{a_{11}+a_{21}} = \frac{N_{00}-N_{10}}{f_1 \cdot N_{00} + N_{10}};\ f_1 = \frac{N_{11}-N_{10}}{N_{00}-N_{01}}$$

  - *Egorov et al.*

    $$A = \begin{pmatrix}a_{11} & 0\\ 0 & a_{22}\end{pmatrix} \Rightarrow p' = \frac{a_{11}}{a_{11}+a_{22}} = \sqrt{p}$$

J. Byrne, NIM A 167, 355 (1999) :

The assumption of Herdin et al.needs to different polarization vector amplitudes between polarizer (p) and analyzer (1).

The assumption of Egorov et al is more natural

⇒ UCN transmission experiment cannot fully distinguish different mechanisms of depolarization

Polarized cold-neutron reflectometry

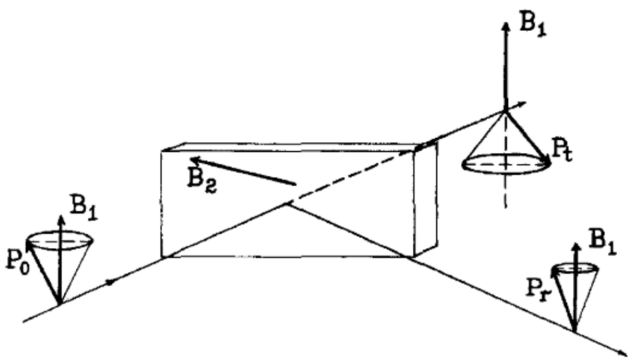

- Early studies on the magnetic materials with cold neutrons
- Reflection on a non-collinear magnetic induction induces depolarization
  → averaged over domains experienced by a neutron

NK. Pleshanov. Z. Phys, B **94**, 233 (1994)

$$\boldsymbol{P} = D(\boldsymbol{n}, \varphi)\, \boldsymbol{P}_0,$$

- Experiment with $Fe_{36}Co_{64}$ film: VM. Pusenkov et al. J. Mag. Mag. Mat. **175** , 237 (1997)
  - Small applied magnetic field: low reflectivity, low polarization of reflected beam
    → increased as the film magnetized

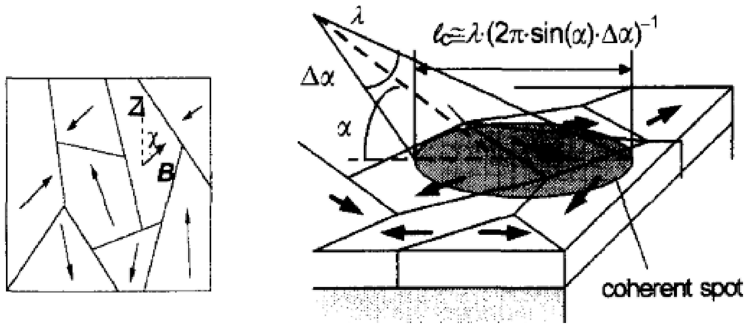

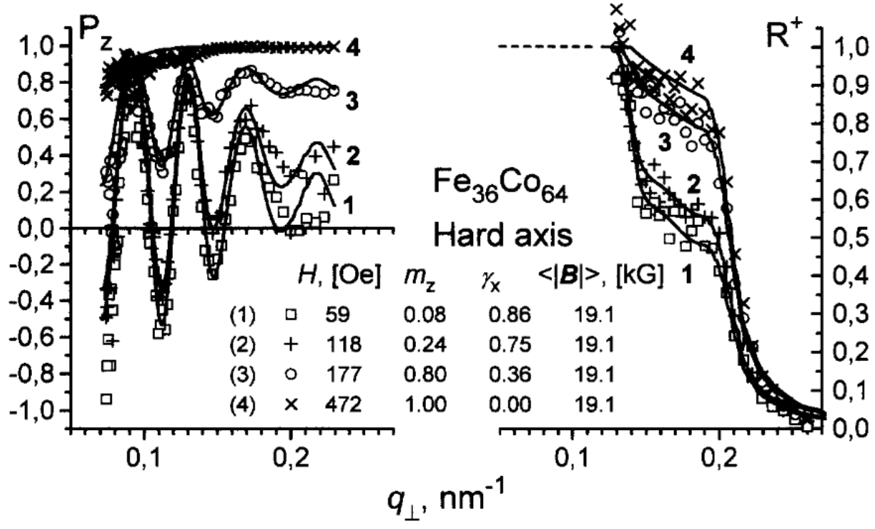

$P_z = (R_{++} - R_{+-})/(R_{-+} + R_{+-})$, $R^{+} = R_{-+} + R_{++}$

⇒ Give complementary information to the UCN measurement (in principle ~$(1 - a_{22})$ of matrix A)

Our strategies

- **Production**
  - In-house ion-beam sputtering at KURNS
    M. Hino et al. NIM A 797,. 265 (2015)
  - Substrate materials:
    Al (t 20–30 um) or Si(t 0.1–2.0 mm)
  - Fe layer thickness: 100–300 nm

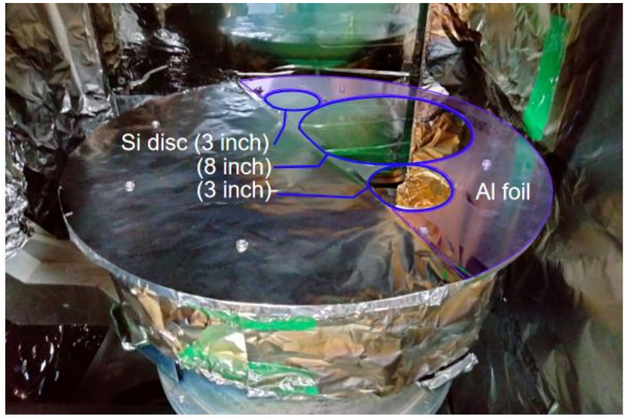

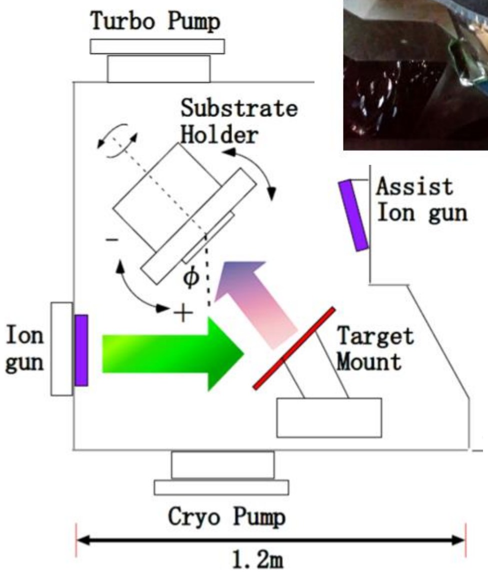

- **Testing**

  UCN transmission
  → Pulsed UCN source at J-PARC
  S. Imajo et al. PTEP **2016**, 013C22 (2016)

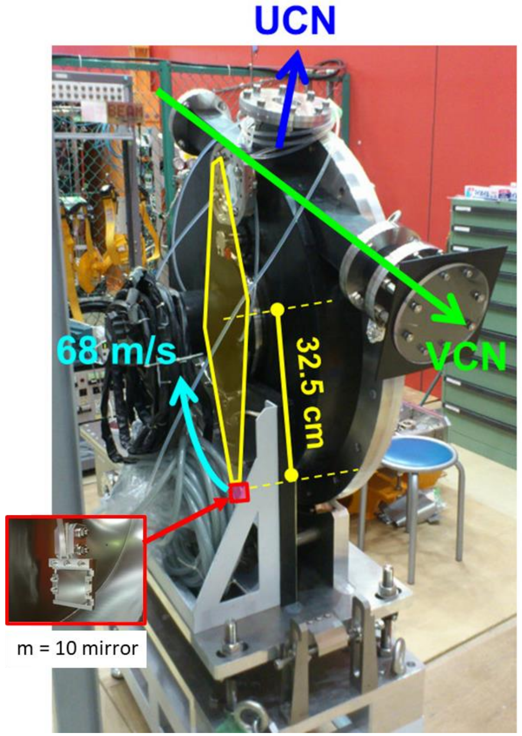

Cold neutron reflectometry (for Si substrate)
→ JRR-3 MINE2
(λ=0.8 nm, Δλ/λ=2.8% monochromatic)

H. Akatsuka et al. JPS Conf. Proc. **37**, 020801 (2022)

Al and Si as substrate for Fe films

	V_F (neV)	σ_{abs} (b) @ 2200 m/s
Al	53.92	0.231
Si	54.21	0.171

- **Si:** mirror-surface wafers available:
  → can be characterized by cold-neutron reflectometry
- **Al:** can be made thin (~20 um) → small absorption
  - Absorption for λ=58 nm (243 neV): Si 0.2 mm: 5.4%, Al 25 um: 1.2%
- **B-H curve measurements by vibrating-sample magnetometry (VSM):**
  Fe on Si saturates more easily than Fe on Al: inverse magnetostriction effects (deformation induces magnetization)

Transmission comparison

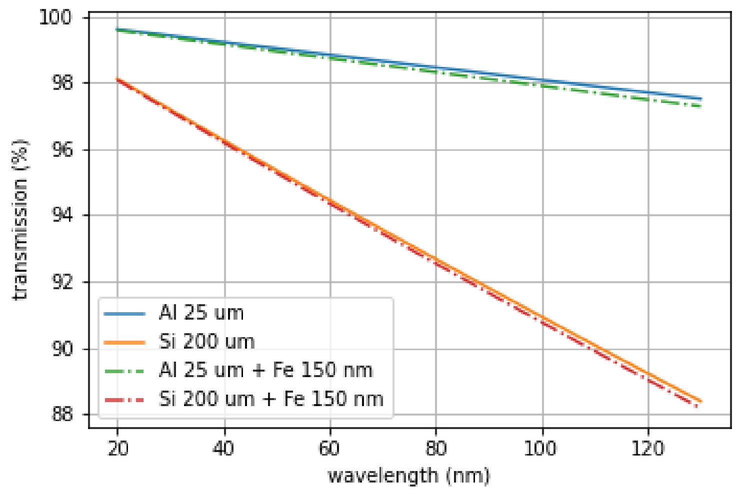

B-H curves

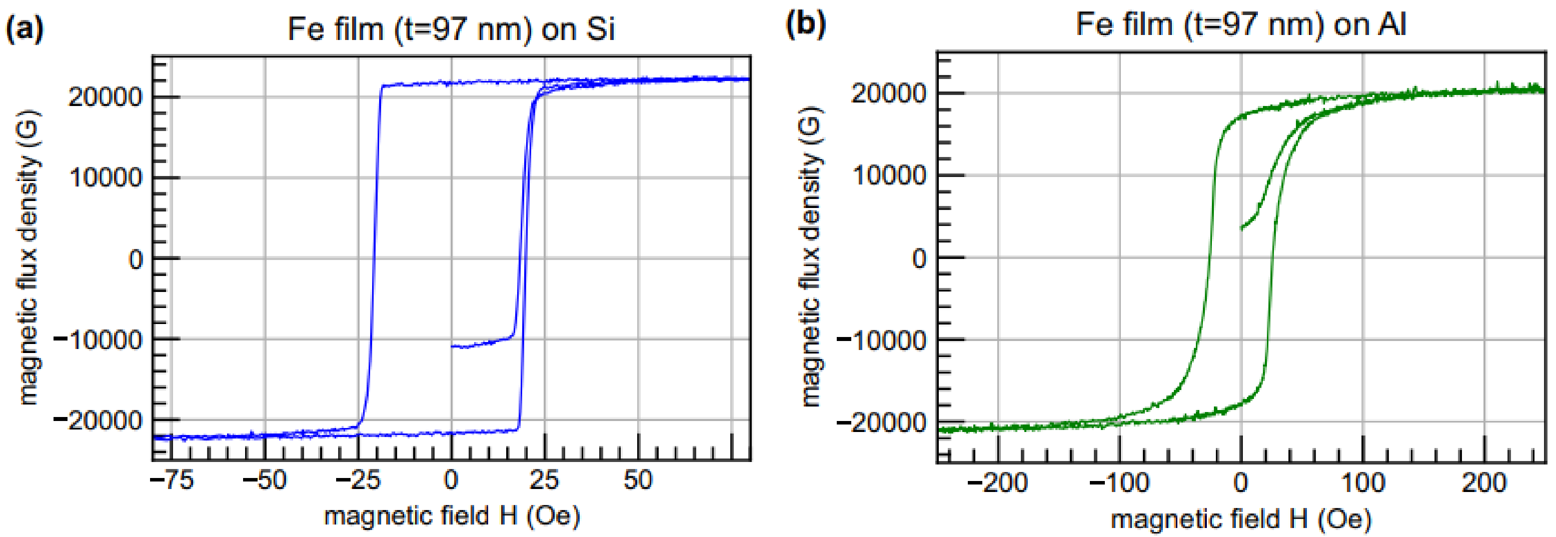

Require ~50 Oe (5 mT) for saturation

Require ~200 Oe (20 mT) for saturation

Outline

- Introduction
    - Principle
    - Review of previous works
    - Our motivations
    - Test methods: UCN transmission measurement, cold-neutron reflectometry
- Recent results
    - UCN measurement at J-PARC
    - Polarized cold-neutron reflectometry measurement at JRR-3
- Summary

Recent results from J-PARC pulsed UCN source

- **Setup:**
  - Doppler shifter produces UCNs every 120 ms
  - Dipole electromagnets (up to 30 mT)
  - Two AFP SFs
- **Samples:**
  - Fe (97 nm) on Al (25 um)
  - Fe (97 nm) on Si (0.2 mm)
- **Results**

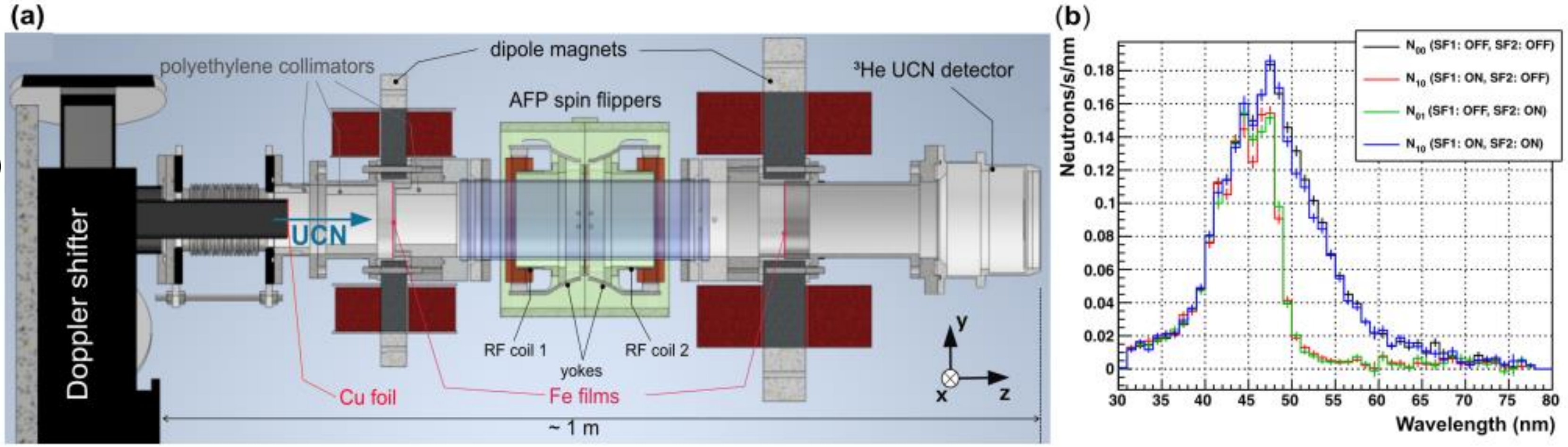

Recent results from J-PARC pulsed UCN source

- **Setup:**
  - Doppler shifter produces UCNs every 120 ms
  - Dipole electromagnets (up to 30 mT)
  - Two AFP SFs
- **Samples:**
  - Fe (97 nm) on Al (25 um)
  - Fe (97 nm) on Si (0.2 mm)

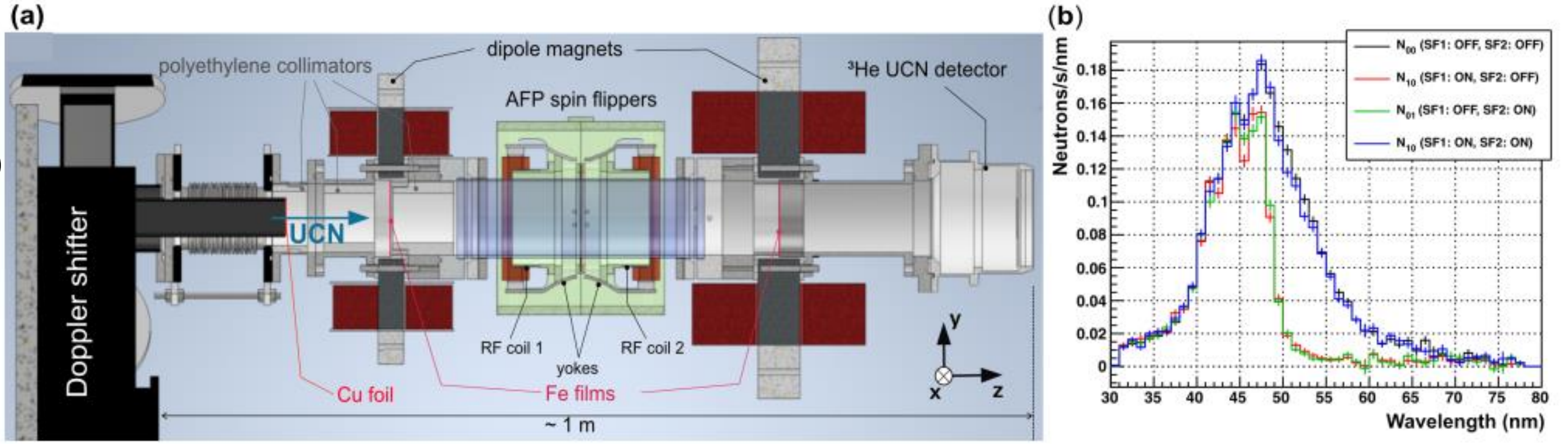

- **Results**

Sample	H (mT)	*p*	*p'*
Fe on Si	6	0.78 (3)	0.88 (1)
Fe on Si	12	0.85 (3)	0.92 (1)
Fe on Si	30	0.86 (3)	0.93 (1)
Fe on Al	12	0.80 (2)	0.89 (1)

*BG neutron counts not fully accounted
→ would increase the polarization value finally

- Rise of *p* between 60 and 120 Oe for Si
- Higher *p* at 120 Oe of Si than Al (more field needed for Al)

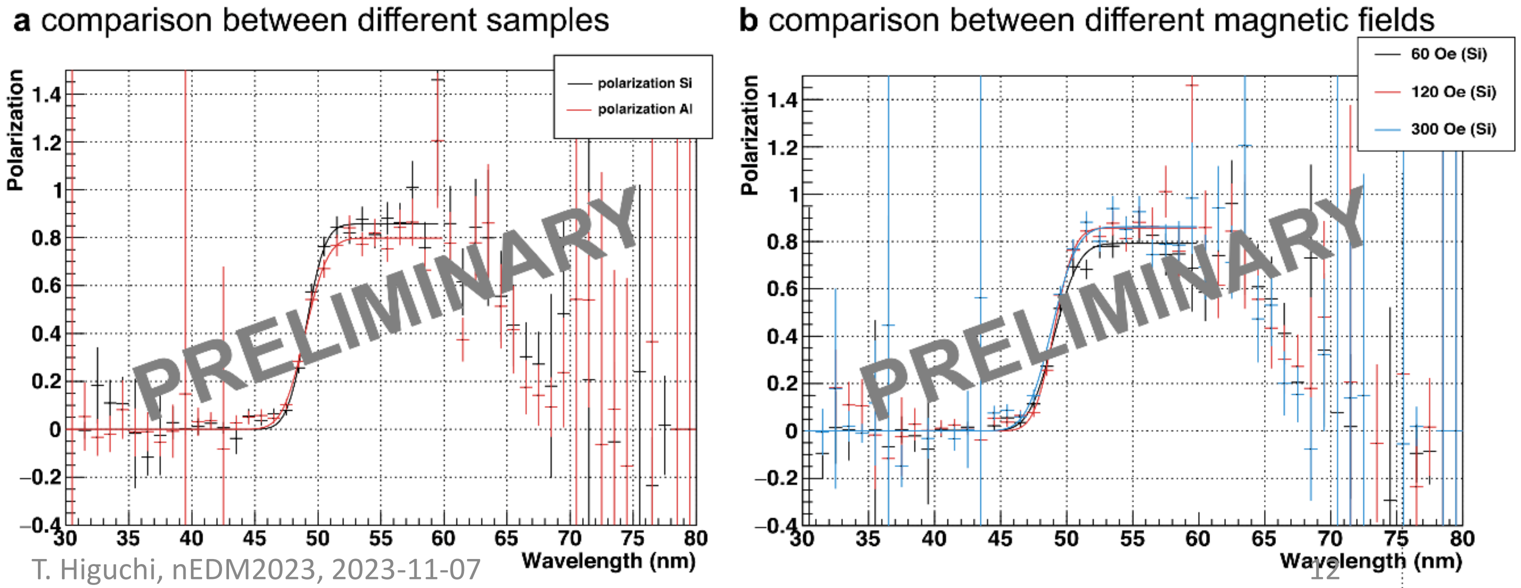

Recent results from JRR-3 MINE2

- **Test setup:**
  - 0.88-nm neutrons polarized by a Fe/SiGe magnetic multilayer mirror to 0.97 polarization
  - Θ-2Θ scan with a rotation stage and a X stage
  - Up to 5.5 mT: used a Helmholtz coil (H)
  - 30 mT: used a magnetic mirror holder (M2)

- **Sample:**
  - Fe (97 nm) on Si (2 mm)

- **Results:**

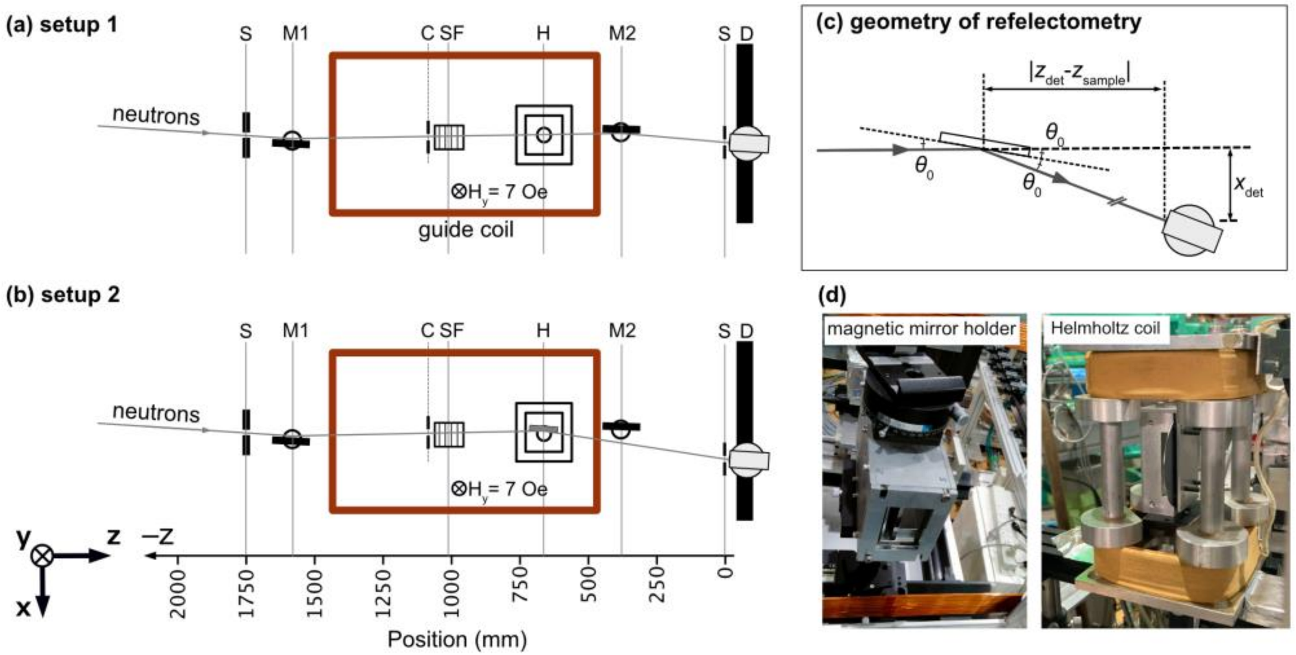

Recent results from JRR-3 MINE2

- **Test setup:**
  - 0.88-nm neutrons polarized by a Fe/SiGe magnetic multilayer mirror to 0.97 polarization
  - Θ-2Θ scan with a rotation stage and a X stage
  - Up to 5.5 mT: used a Helmholtz coil (H)
  - 30 mT: used a magnetic mirror holder (M2)

- **Sample:**
  - Fe (97 nm) on Si (2 mm)

- **Results:**
  - Data with spin on/off simultaneous fitted with a model
  - The reflectivity in different applied magnetic fields

H (mT)	R_0
1.7	0.86 (6)
2.5	0.87 (7)
3.2	0.89 (7)
5.5	0.88 (6)
30	0.95 (9)

Rise of reflectivity between 5.5 and 30 mT

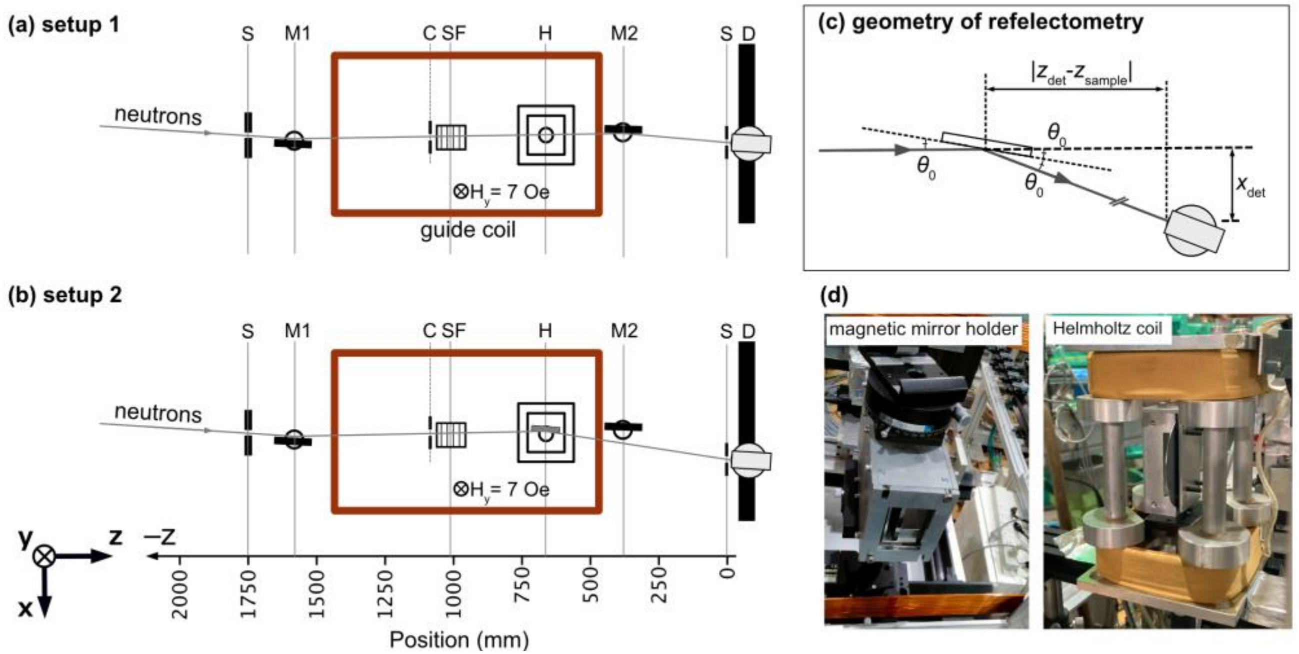

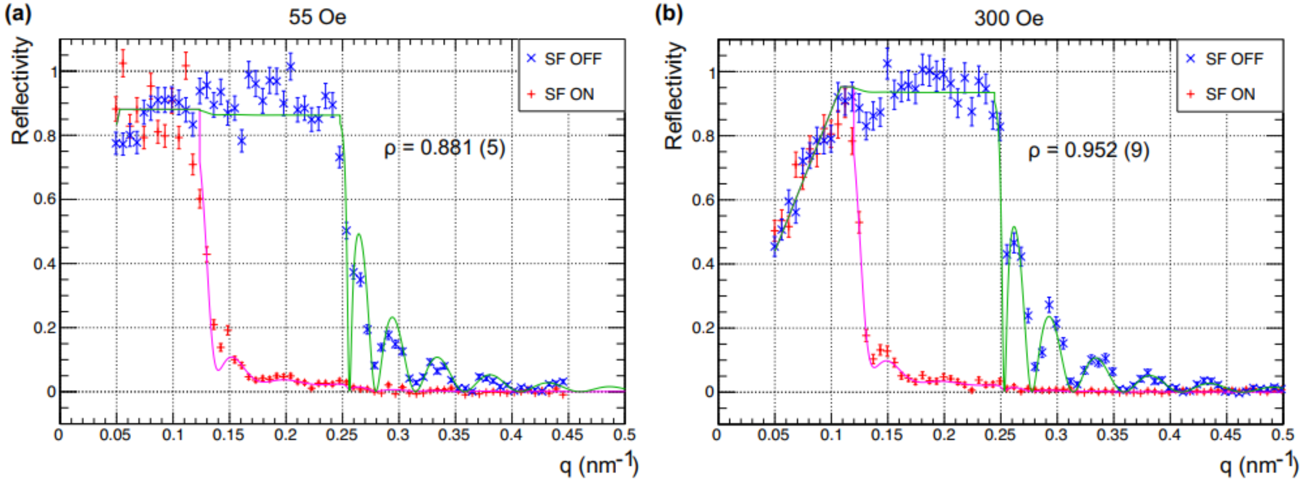

Summary

- Introduced polarized cold-neutron reflectometry as a testing method of Fe films complementary to UCN transmission measurement
- Preliminary results imply that the magnetic field required to operate Si-substrate Fe film is larger than 5 mT as indicated by VSM
- Spin-analyzers for TUCAN EDM experiment: films with analyzing efficiency of 90% (12 mT) developed. Further evaluation & development planned

More details will be on: T. Higuchi et al. J. Phys. Soc. Jpn. (submitted)

Acknowledgements

JST-funded PhD position(s) available at Kyoto U.!

Thank you for your attention!

Backup

MINE2 polarized cold-neutron reflectometry

- Fit model

$$R(q|q_{1,\pm}, q_2, d) = \begin{cases} 1 & (q < q_{1,\pm}) \\ \left| \dfrac{r_{10} - r_{12}\exp(iq_{1,\pm}d)}{1 - r_{12}r_{10}\exp(iq_{1,\pm}d)} \right|^2 & (q \geq q_{1,\pm}) \end{cases}$$

$$\text{with} \quad r_{10} \equiv \frac{q - q_{1,\pm}}{q + q_{1,\pm}}, \; r_{12} \equiv \frac{q_2 - q_{1,\pm}}{q_2 + q_{1,\pm}}. \qquad (15)$$

$$q_{1,\pm} = \sqrt{q^2 - \frac{8m_n V_{\mathrm{eff},\pm}}{\hbar^2}}, \; q_2 = \sqrt{q^2 - \frac{8m_n V_{\mathrm{Si}}}{\hbar^2}}.$$

$R(q|q_{1,\pm}, q_2, d)$ by

$$R_0 = \frac{1 + p_3}{2} R(q|q_{1,+}, q_2, d) + \frac{1 - p_3}{2} R(q|q_{1,-}, q_2, d)$$

$$R_1 = \frac{1 - p_3}{2} R(q|q_{1,+}, q_2, d) + \frac{1 + p_3}{2} R(q|q_{1,-}, q_2, d).$$

$$\eta(q|q_{\mathrm{th}}) = \begin{cases} q/q_{\mathrm{th}} & (q < q_{\mathrm{th}}) \\ 1 & (q \geq q_{\mathrm{th}}). \end{cases}$$

$$R'_0(q|q_{1,+}, q_{1,-}, q_2, q_{\mathrm{th}}, d, p, \rho) = \rho\eta(q|q_{\mathrm{th}}) \left[\frac{1 + p_3}{2} R(q|q_{1,+}, q_2, d) + \frac{1 - p_3}{2} R(q|q_{1,-}, q_2, d) \right], \qquad (18)$$

$$R'_1(q|q_{1,+}, q_{1,-}, q_2, q_{\mathrm{th}}, d, p, \rho) = \rho\eta(q|q_{\mathrm{th}}) \left[\frac{1 - p_3}{2} R(q|q_{1,+}, q_2, d) + \frac{1 + p_3}{2} R(q|q_{1,-}, q_2, d) \right]. \qquad (19)$$

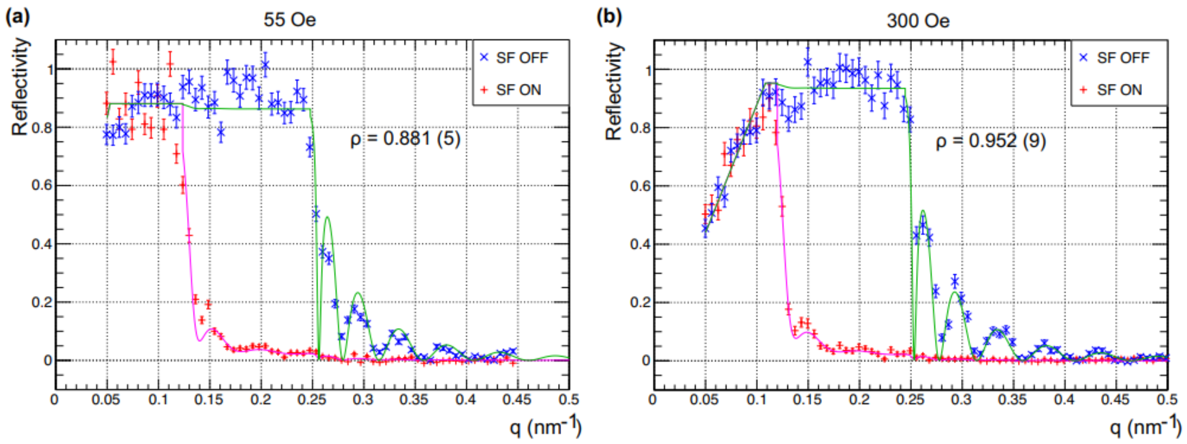

MINE2 polarized cold-neutron reflectometry

- Fit results

H (Oe)	$q_{1,+}$ (nm^{-1})	$q_{1,-}$ (nm^{-1})	q_2 (nm^{-1})	q_{th} (nm^{-1})	d (nm)	ρ	p_3	χ^2/ndf
17	0.1275 (4)	0.2472 (1)	0.117 (3)	0.059 (1)	96.5 (2)	0.855 (5)	0.935 (4)	855/123
25	0.2470 (1)	0.1225 (7)	0.109 (7)	0.052 (1)	96.1 (2)	0.870 (6)	0.891 (5)	808/123
32	0.2475 (1)	0.1255 (6)	0.110 (7)	0.058 (1)	97.8 (2)	0.890 (6)	0.910 (4)	838/123
55	0.2479 (1)	0.124 (2)	0.110 (2)	0.053 (2)	97.2 (2)	0.881 (5)	0.958 (4)	918/123
300	0.2445 (2)	0.1200 (5)	0.110 (4)	0.108 (2)	95.5 (3)	0.952 (9)	0.962 (4)	394/139

VM. Pusenkov et al. J. Mag. Mag. Mat. 175 , 237 (1997)

$$\boldsymbol{P} = D(\boldsymbol{n}, \varphi)\, \boldsymbol{P}_0,$$

$$\varphi = \varphi_+ - \varphi_-,$$

$$\varphi_+ = 2 \arccos\{[E_\perp / V^+]^{1/2}\} \quad (E_\perp < V^+),$$

$$\varphi_- = 2 \arccos\{[E_\perp / V_g]^{1/2}\} + 2k_\perp d$$

$$(V^- < E_\perp < V_g).$$

$$P_z = D_{zz} = \langle 1 - n_x^2\,(1 - \cos(\varphi))\rangle.$$

$$m_z \equiv \langle n_z \rangle = \langle f(\chi) \cos(\chi) \rangle = \langle B_z \rangle / B,$$

$$\gamma_x \equiv \langle n_x^2 \rangle = (1 - \langle f(\chi) \cos(2\chi) \rangle)/2.$$

$$R^+ = R_{-+} + R_{++} \cong \langle \cos^2(\chi/2) \rangle = \tfrac{1}{2}(1 + m_z), \quad (9a)$$

$$P_z \cong 1 - \tfrac{1}{2} \langle \sin^2(\chi) \rangle \langle \cos^{-2}(\chi/2) \rangle$$

$$= 1 - \gamma_x/(1 + m_z). \qquad (9b)$$

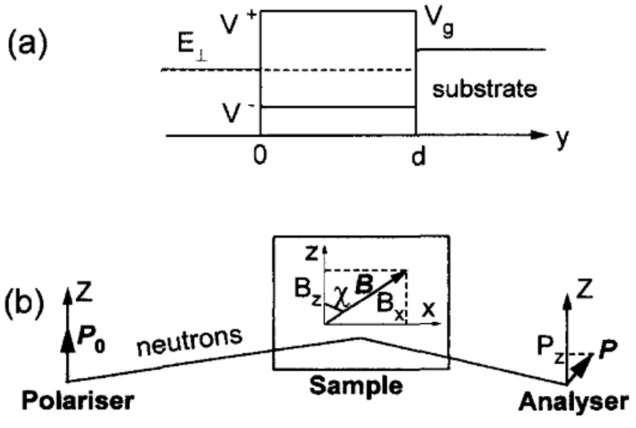

Fig. 1. (a) The potentials of a magnetic film. (b) The experimental scheme. The directions of the quantisation axis (Z), the guide field ($\boldsymbol{H}$), and the magnetic induction in the film ($\boldsymbol{B}$) are shown; the coordinate system (x, y, z) is connected with the sample.

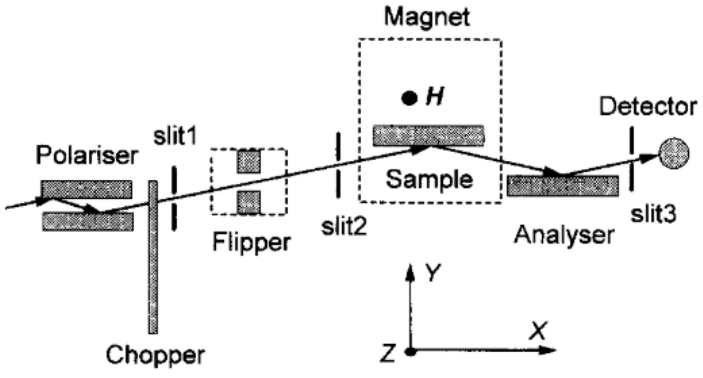

Fig. 4. A scheme of the neutron reflectometer ZINA.

J. Byrne, NIM A 167, 355 (1999)

- Introduced 3-dimensional polarization vector (<-> Stokes vector of light polarization)
- Re-formulate the transfer matrix in three-dimensional form, T: polarizer/analyzer, R: spin flipper

$$P_0 = I, \qquad \boldsymbol{P} = P_0 \langle \boldsymbol{\sigma} \rangle = \boldsymbol{P}_0 \boldsymbol{p}$$

$$P' = TP$$

$$\boldsymbol{p}_p = \frac{T_{x0}}{T_{00}}, \frac{T_{y0}}{T_{00}}, \frac{T_{z0}}{T_{00}}. \qquad \boldsymbol{p}_a = \frac{T_{0x}}{T_{00}}, \frac{T_{0y}}{T_{00}}, \frac{T_{0z}}{T_{00}}.$$

$$R = \begin{pmatrix} 1 & 0 \\ 0 & M \end{pmatrix}$$

$$P' = TRTP$$

$$P_0'(0, \phi) = C_1 \quad \text{and} \quad P_0'(\pi, \phi) = C_2$$

$$\frac{C_1 - C_2}{C_1 + C_2} = \frac{T_{z0} T_{0z}}{T_{00}^2} = \boldsymbol{p}_p \cdot \boldsymbol{p}_a .$$

The result [eq. (1)] of Egorev et al.[2]) follows immediately from the assumption $\boldsymbol{p}_p \equiv \boldsymbol{p}_a$ whereas the results of Herdin et al.[2]) hold only in the limit that $\boldsymbol{p}_a$ and $\boldsymbol{p}_p$ are parallel and that $|\boldsymbol{p}_a| \equiv 1$. This implies that the active element, although an imperfect polarizer is yet a perfect analyser. Such a notion, although tenable in theory, seems somewhat unlikely in practice. Indeed one might comment that, since Herdin et al.[1]) limit their discussion to a formulation in terms of 2×2 transfer matrices, effectively suppressing the x and y components of the polarization, the possible non-parallelism of $\boldsymbol{p}_a$ and $\boldsymbol{p}_p$ lies outside the range of their treatment.

Kim & Oliveria, J. Appl. Phys. 74, 1233–1241 (1993)

- Dependence of magnetic properties of sputtered Fe film

Critical thickness δ:

$\delta \sim \sqrt{A/K}$

A: exchange stiffness,

K: magnetic anisotropy constant

For Fe, $\delta \sim 40\,\text{nm}$

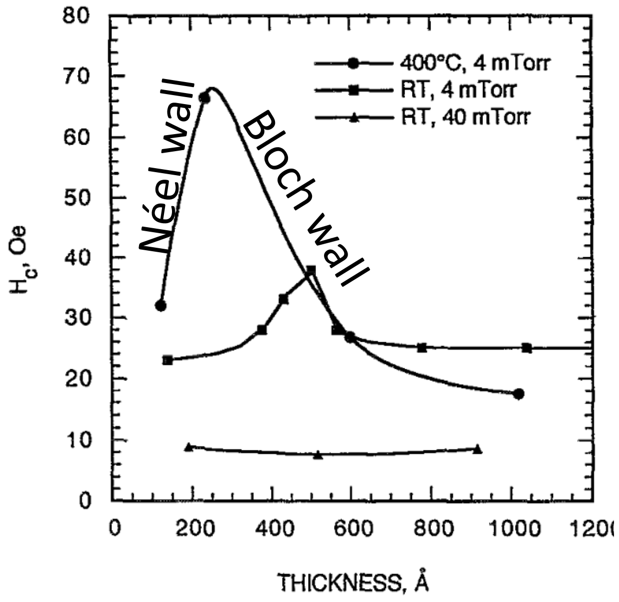

FIG. 11. Coercivity, H_c, as a function of film thickness.

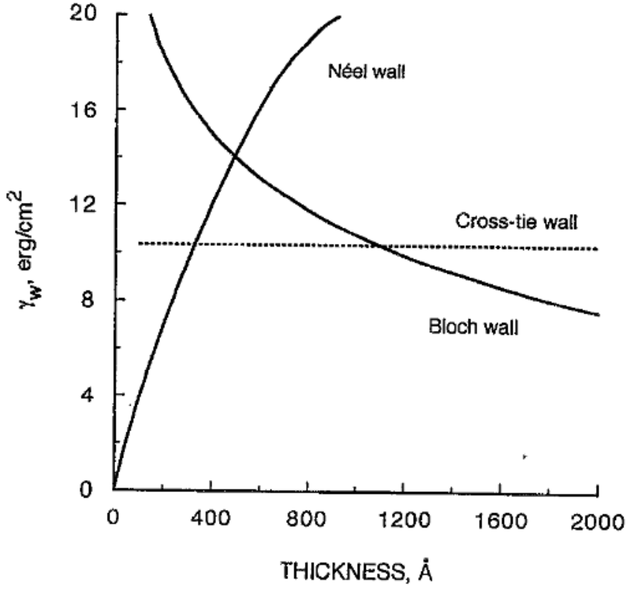

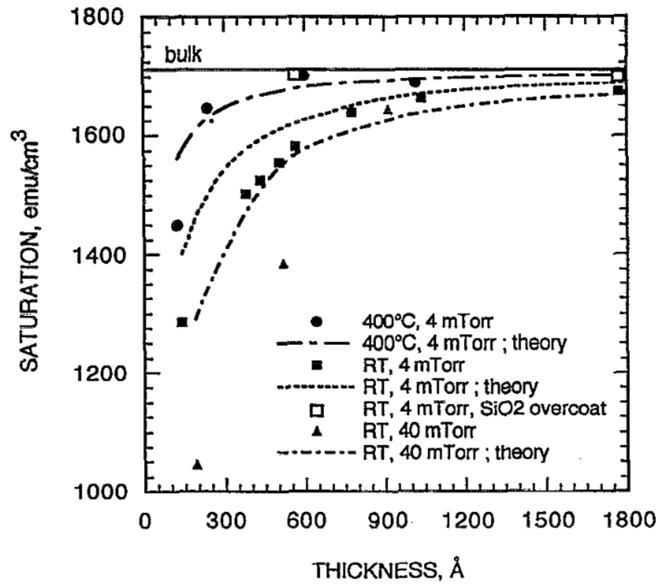

FIG. 4. Saturation magnetization, M_s, as a function of film thickness.

$$M_s^{tot}(\text{theory}) = pM_s^{Fe}(\text{bulk}) + (1-p)M_s^{Fe_3O_4}(\text{bulk})$$

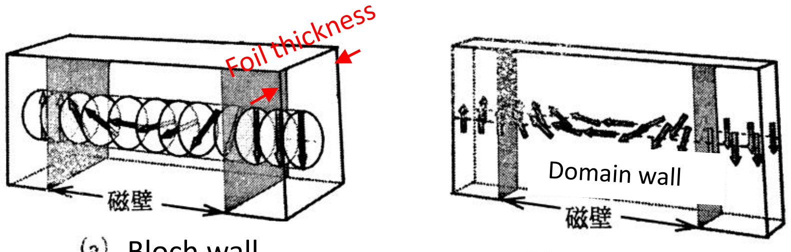

(a) Bloch wall (b) Néel wall

M. Prutton, Thin Ferromagnetic Films (Buttenvorths, London, 1964)